Dual Energy Imaging

Sabee Molloi, Ph.D.

University of California
Department of Radiological Sciences
Irvine, California

DISCLOSURES

- Toshiba
- Philips

Outline

- Introduction
- Dual energy mammography
- Spectral mammography
- Dual energy breast CT
- Spectral breast CT
- Conclusion

Dual Energy Imaging

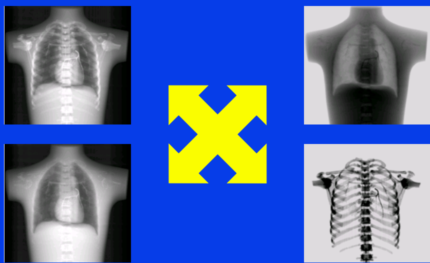

Dual Energy Mammography

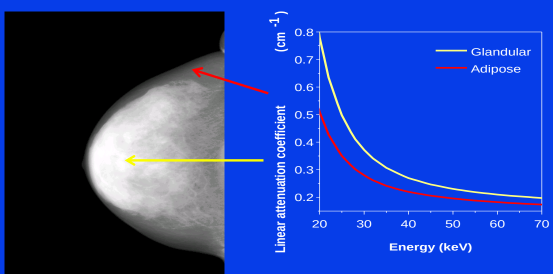

Dual Energy Decomposition

$l = l(t_g, t_a)$ $h = h(t_g, t_a)$

$t_g = t_g(l,h)$ $t_a = t_a(l,h)$

$$t_i = \frac{a_0 + a_1 l + a_2 h + a_3 l^2 + a_4 lh + a_5 h^2}{\sqrt{1 + b_1 l + b_2 h}}$$

Ducote J L , Molloi S, Quantification of breast density with dual energy mammography: An experimental feasibility study, Med. Phys. 37: 793, 2010.

Outline

- Introduction
- Dual energy mammography
- Spectral mammography
- Dual energy breast CT
- Spectral breast CT
- Conclusion

Dual energy Mammography

- Hologic Selenia Digital Mammography
- Tungsten anode x-ray tube.
- 28 kVp, 60 mAs, 50 µm rhodium filter.
- 49 kVp, 30 mAs, 300 µm copper filter.
- Scatter correction.

Dual kVp Mammography

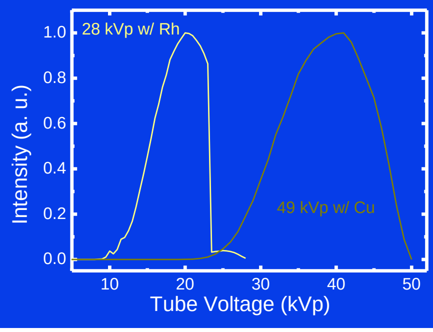

Breast density

Mammographically dense breast has been shown to be strongly associated with breast cancer risk[1]

1. Boyd, et al. J National Cancer Inst, 87. p670-675, 1995.

Breast density

$$\text{Breast Density} = \frac{t_g}{t_g + t_a} \text{x}100$$

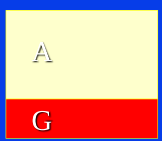

Breast Tissue Study

- 20 postmortem breast pairs
- BI-RADS ranking by 3 radiologists
- Standard grey level thresholding
- Dual energy mammography
- Chemical analysis

Chemical Analysis

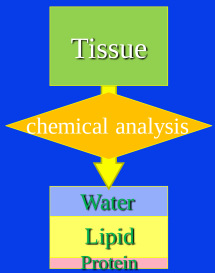

1. Evaporate water in vacuum oven
2. Dissolve lipid in petroleum ether
3. Remove protein using vacuum filtration

Fibroglandular Volume Fraction

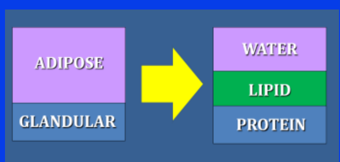

$$\%FGV x100 = \frac{V_W + V_P}{V_W + V_L + V_P}$$

Right-left Breast Correlation from Chemical Analysis

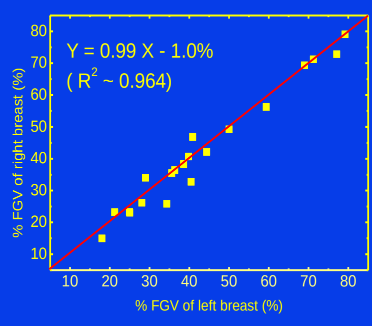

Visual estimation

Breast Imaging Reporting and Data System (BI-RADS)

BI-RADS 1-4 with increasing level of glandularity.

BI-RADS Rankings by Radiologists

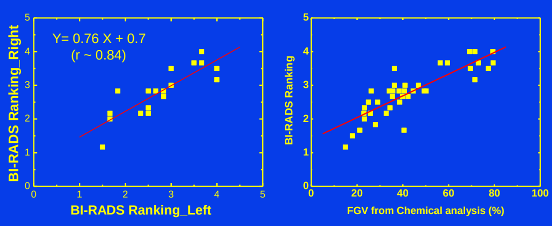

Gray level thresholding

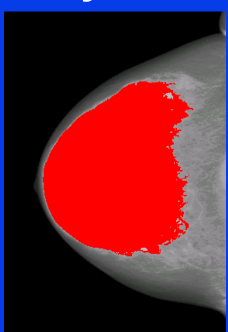

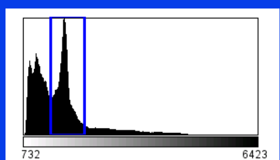

Gray Level Thresholding

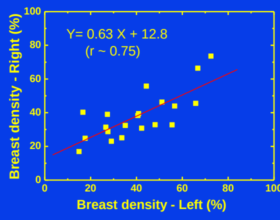

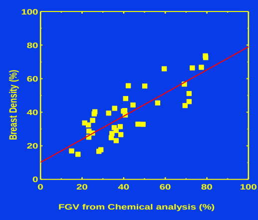

Dual Energy Mammography

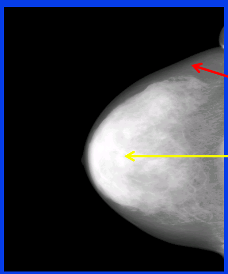

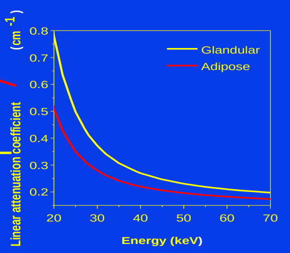

Dual energy material decomposition

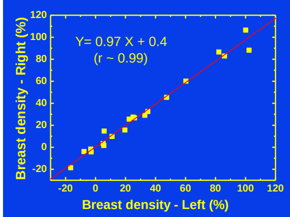

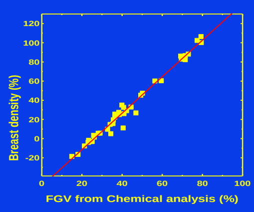

Breast Density Variability

	Bi-RADS	Thresholding	Dual Energy
Right - Left	2.0	2.0	1.0
Chemical Analysis	2.1	1.8	1.0

Outline

- Introduction
- Dual energy mammography
- Spectral mammography
- Dual energy breast CT
- Spectral breast CT
- Conclusion

Spectral Mammography

- Philips MicroDose SI Digital Mammography
- Tungsten anode x-ray tube.
- Equivalent filtration 0.75 mm of Al.
- Noise floor 8.7 keV.
- No scatter correction.

Spectral mammography system

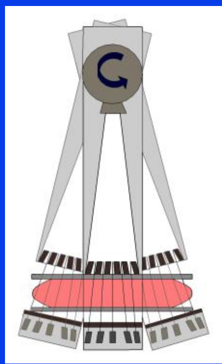

Spectral Mammography

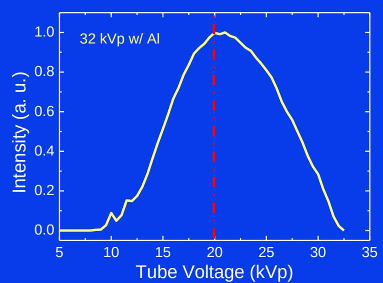

Human Study

- 93 mammography patients
- BI-RADS ranking by 10 radiologists (5 US, 5 UK)
- Standard grey level thresholding (Cumulus)

Examples of Spectral Mammography images

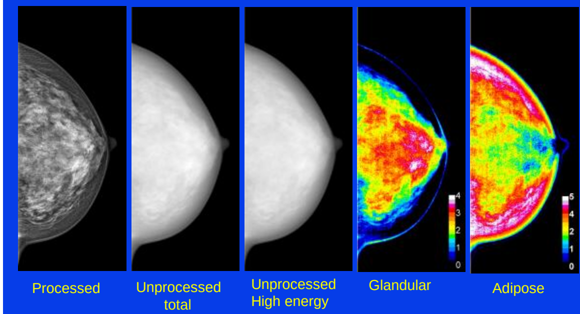

BI-RADS Rankings by Radiologists

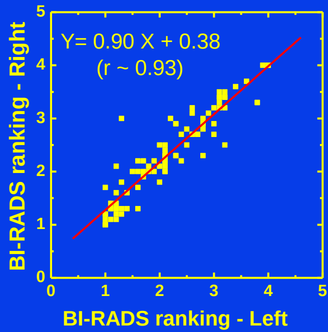

Grey Level Thresholding

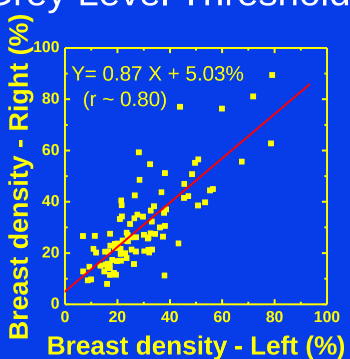

Spectral material decomposition

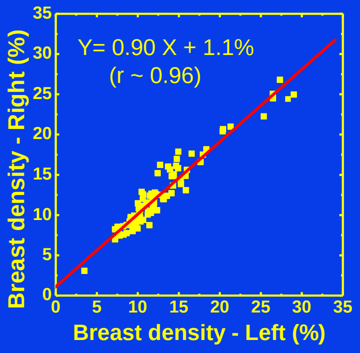

Breast Density Variability

	Bi-RADS	Thresholding	Spectral
Right - Left	2.0	2.9	1.0

Outline

- Introduction
- Dual energy mammography
- Spectral mammography
- Dual energy breast CT
- Spectral breast CT
- Conclusion

Dual energy breast CT

- 20 pairs of postmortem breasts
- Varian 4030CB on optical bench
- Scatter-glare and beam hardening Corrections

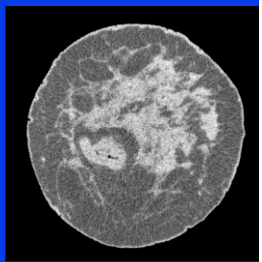

Dual Energy Decomposition

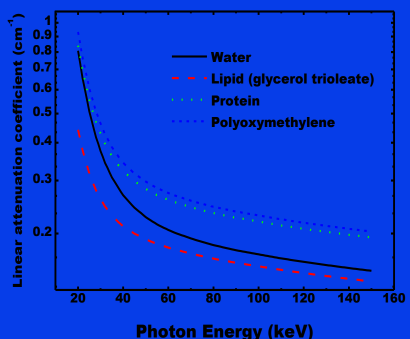

Dual energy CT

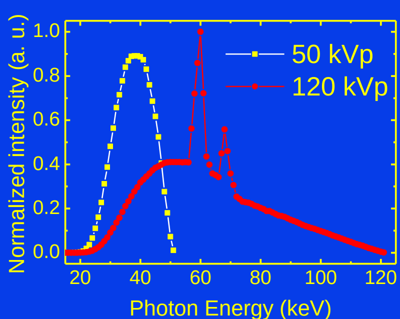

Calibration phantom

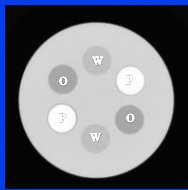

Water → Water
Oil → Lipid
Delrin plastic (Polyoxymethylene) → Protein

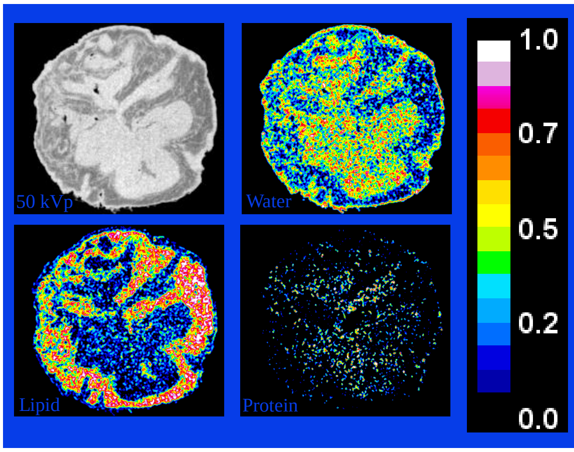

Accuracy of Volumetric Water Fraction

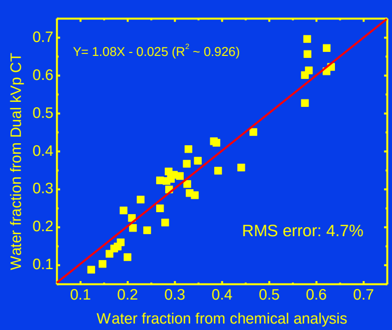

Accuracy of Volumetric Lipid Fraction

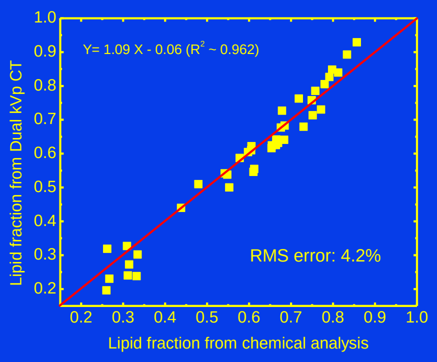

Accuracy of Volumetric Protein Fraction

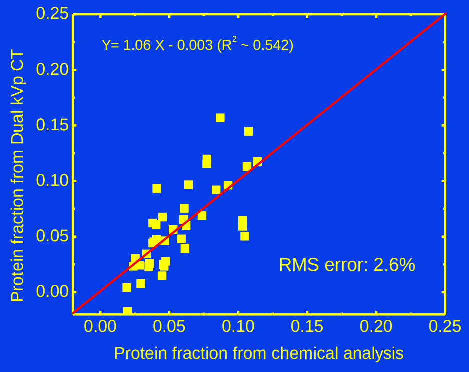

Outline

- Introduction
- Dual energy mammography
- Spectral mammography
- Dual energy breast CT
- Spectral breast CT
- Conclusion

Spectral breast CT

- 20 pairs of postmortem breasts
- eV 2500 CZT on optical bench
- Spectral distortion corrections

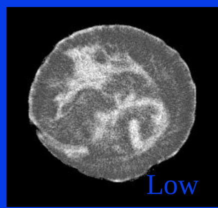

Rotation and translation stage

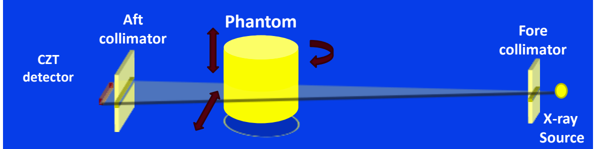

Spectral breast CT

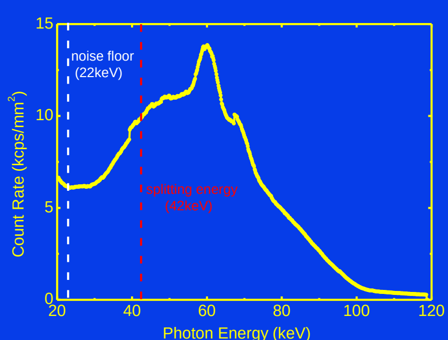

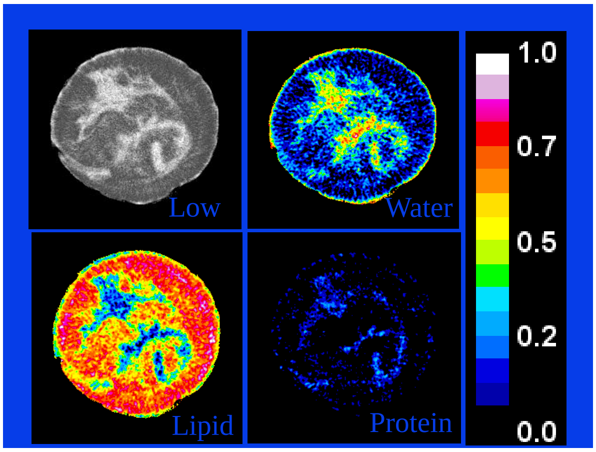
Low
Water
Lipid
Protein
1.0
0.7
0.5
0.2
0.0

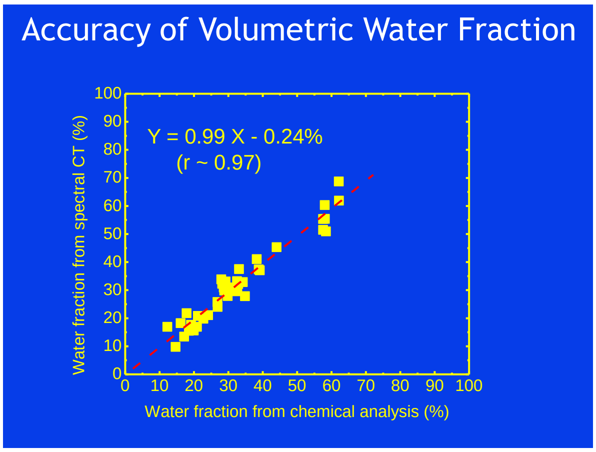
Accuracy of Volumetric Water Fraction
Y = 0.99 X - 0.24%
(r ~ 0.97)
Water fraction from spectral CT (%)
Water fraction from chemical analysis (%)
0 10 20 30 40 50 60 70 80 90 100

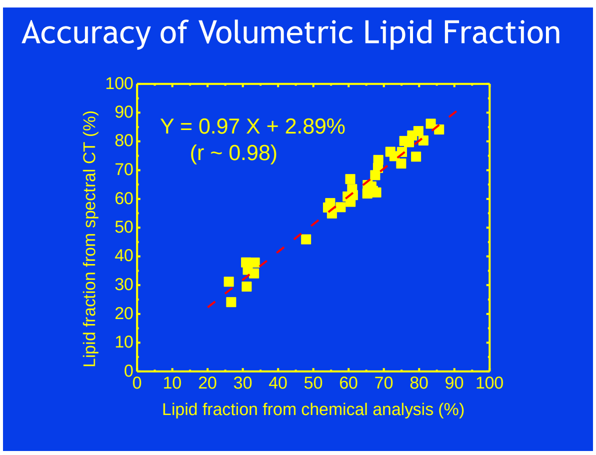
Accuracy of Volumetric Lipid Fraction
Y = 0.97 X + 2.89%
(r ~ 0.98)
Lipid fraction from spectral CT (%)
Lipid fraction from chemical analysis (%)
0 10 20 30 40 50 60 70 80 90 100

Accuracy of Volumetric Protein Fraction

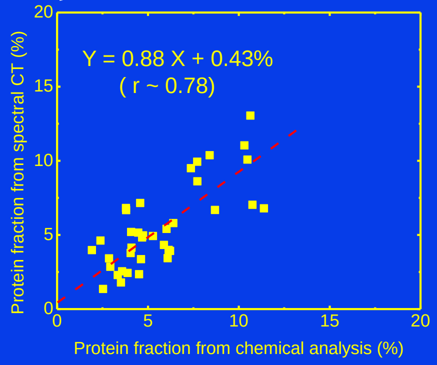

Outline

- Introduction
- Dual energy mammography
- Spectral mammography
- Dual energy breast CT
- Spectral breast CT
- Conclusion

Conclusions

- Dual energy imaging can be used to accurately quantify breast density or water, lipid, and protein contents in breast tissue.
- It can potentially improve breast cancer diagnosis.

ACKNOWLEDGMENTS

This research was supported in part by Grant No. R01 CA136871 awarded by the NCI, DHHS.

X-ray Imaging Physics Laboratory

Huanjun Ding, Ph.D.
Hyo Min Cho, Ph.D.
Benjamin Ziemer, Ph.D.
Bahman Sadeghi, M.D.
Hanna Javan, M.D.

Graduate Students:
Logan Hubbard, M.D./Ph.D. student
Nikita Kumar

Collaborators:
Stephen Feig, M.D.
Carlos Iribarren, M.D., MPH, Ph.D.

Right-left Breast Correlations

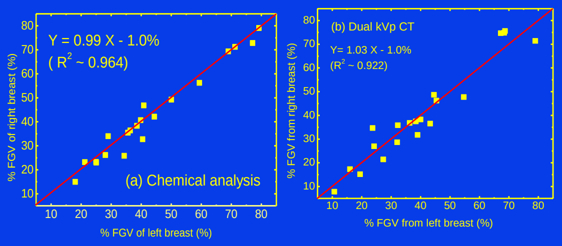

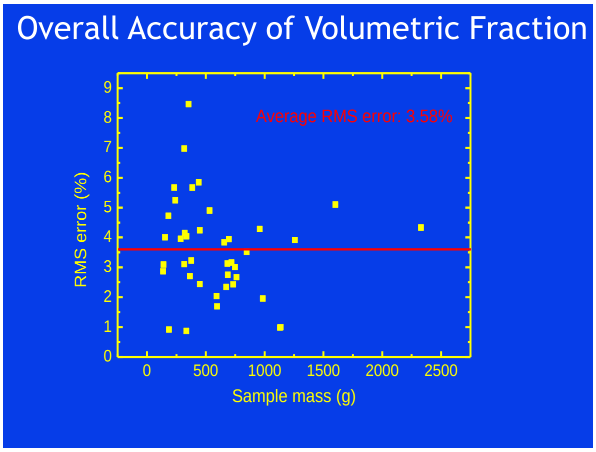
Overall Accuracy of Volumetric Fraction
Average RMS error: 3.58%
RMS error (%)
Sample mass (g)
0
500
1000
1500
2000
2500

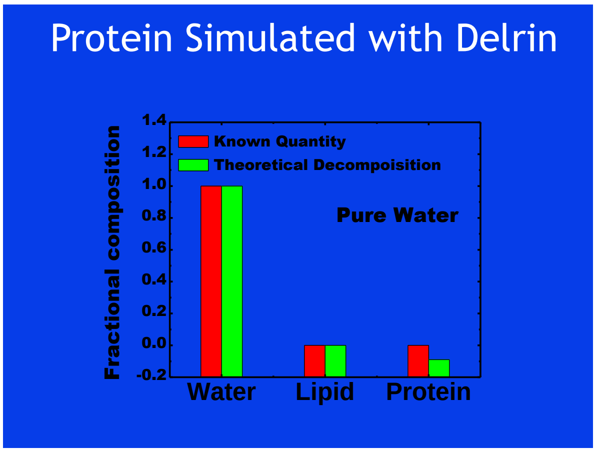
Protein Simulated with Delrin
Known Quantity
Theoretical Decompoisition
Pure Water
Fractional composition
Water
Lipid
Protein

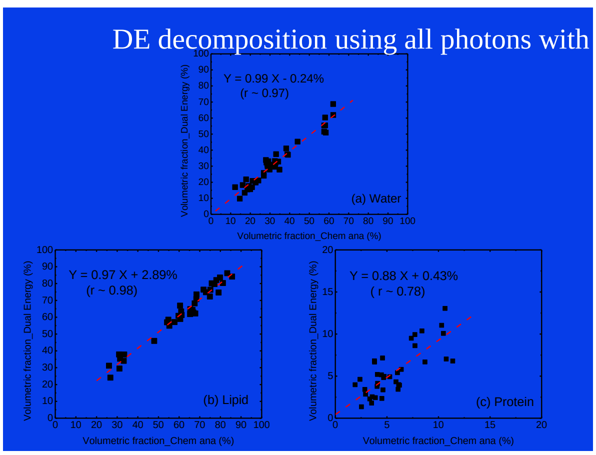
DE decomposition using all photons with
Y = 0.99 X - 0.24%
(r ~ 0.97)
(a) Water
Volumetric fraction_Dual Energy (%)
Volumetric fraction_Chem ana (%)
Y = 0.97 X + 2.89%
(r ~ 0.98)
(b) Lipid
Volumetric fraction_Dual Energy (%)
Volumetric fraction_Chem ana (%)
Y = 0.88 X + 0.43%
(r ~ 0.78)
(c) Protein
Volumetric fraction_Dual Energy (%)
Volumetric fraction_Chem ana (%)

Protein Simulated with Delrin

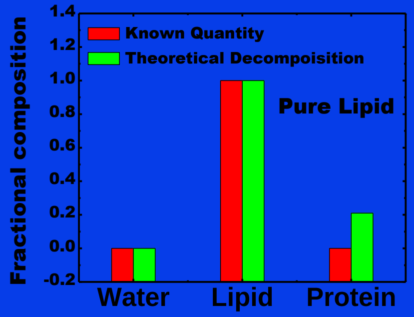

Protein Simulated with Delrin

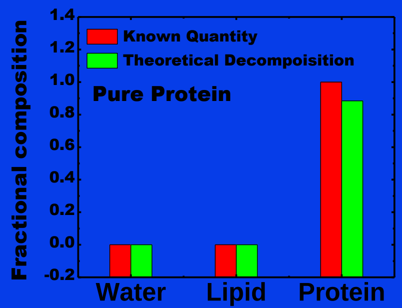

Introduction

- Breast tissue compositional information may improve breast cancer diagnosis.
- Water content of tissue is affected by pathology.

Goal

Validate dual energy CT for decomposition of breast tissue into water, lipid and protein using chemical analysis as the gold standard.

Conclusions

- The high correlation of Breast Density with respect to data from chemical analysis validates the use of dual energy mammography as an accurate measurement of breast tissue composition.

Conclusions

- Variability of breast density measurement is reduced by a factor of two as compared with BI-RADS ranking.
- Spectral mammography is expected to further enhance utility of breast density as a risk factor for breast cancer.

Goal

Develop a quantitative method to measure breast tissue composition in terms of water, lipid and protein using spectral CT

Outline

- Introduction
- Simulation studies
- Physical phantom studies
- Postmortem breast studies

Introduction

Mammographically dense breast has been shown to be strongly associated with breast cancer risk[1]

1 Boyd, et al. J National Cancer Inst, 87. p670-675, 1995.

Introduction

Assessing breast density using pattern classification and visual estimation

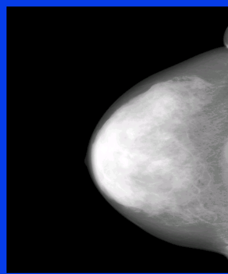

Introduction

Breast density is defined as the percentage of glandular breast tissue

$$Breast\ Density = \frac{G}{G + A} x100$$

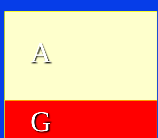

Introduction

Two-tissue assumption and three compartment model for breast.

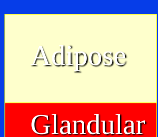

Introduction

Three compartmental model of breast

- Lesion characterization according to their composition[1]
- Water content of tissue is affected by pathology

1. A. D. Laidevant, S. Malkov, C. I. Flowers, K. Kerlikowske and J. A. Shepherd, "Compositional breast imaging using a dual-energy mammography protocol," Med Phys **37**, 164-174 (2010).

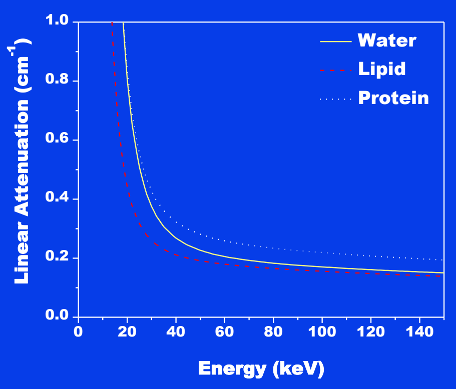

Outline

- Introduction
- Simulation studies
- Physical phantom studies
- Postmortem breast studies
- Patient studies

Simulation Model

Analytical model to calculate optimal figure of merit (FOM)

FOM=SNR/

- Details

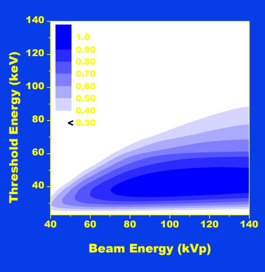

Theoretical Analysis I
WLP -> WLP
(mean) energies of 50 kVp and 120 kVp

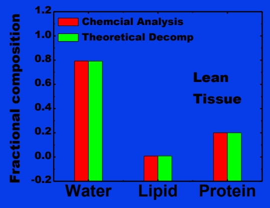

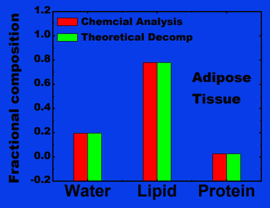

Theoretical Analysis I
WLD -> WLP

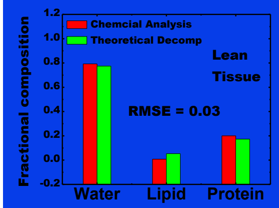

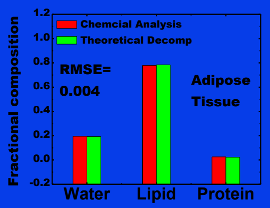

Theoretical Analysis II
WLD Calibration -> …

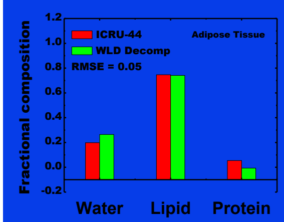

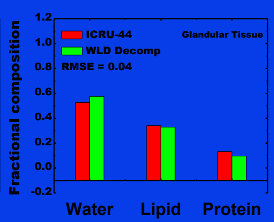

Theoretical Analysis II
WLD Calibration -> …

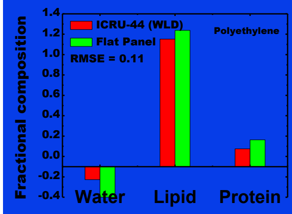

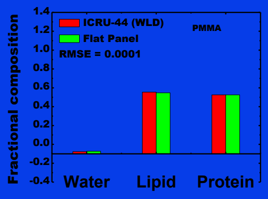

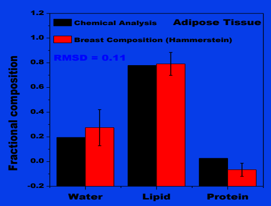

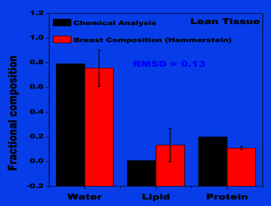

Outline

- Introduction
- Simulation studies
- Physical phantom studies
- Postmortem breast studies
- Patient studies

oton counting and energy resolving detect

- Photon counting
- Energy resolving
- Electronic noise rejection
- Examples: CdZnTe crystals

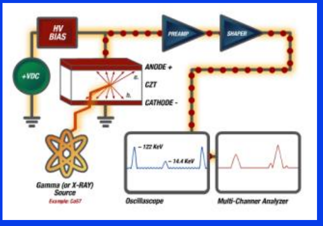

eV 2500 – eV Microelectronics

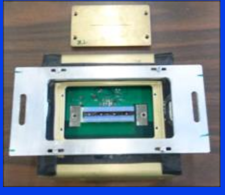

CdZnTe (CZT) crystals
4 crystals, 64 pixels
51.2 mm total length
0.8 mm pitch
5 energy bins

Small field-of-view prototype

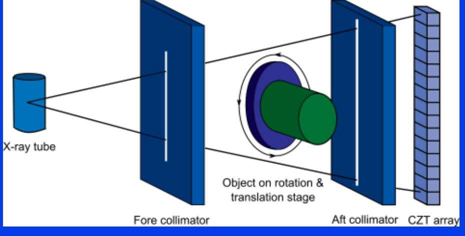

Experiment

Beam energy: 100 kVp
Threshold energy: 40 keV (meat), 42 keV (post-mortem breast samples)
Current: 1.0 mA
Scan time: 61.5 s/rotation
Scan mode: 2D (meat), 3D Helical (post-mortem breast samples)
Filtration: 1 mm Al (meat), 2 mm Al (post-mortem breast samples)
Dose: 3.74 mGy (meat), 1.75 mGy (post-mortem breast samples)

Phantom study

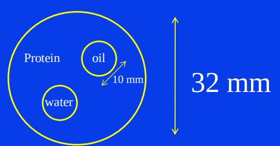

Bin1 (22 ~ 40 keV) Bin2 (40 ~ 100 keV)

Three material decomposition on pl

ROI	Water		Oil		Protein	
	measured	expected	measured	expected	measured	expected
1	55.5%	50%	-3.9%	0%	48.3%	50%
2	3.3%	0%	48.7%	50%	47.9%	50%
3	9.1%	10%	13.7%	10%	77.3%	80%

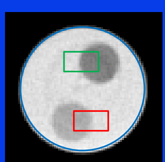

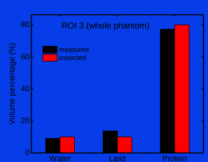

Outline

- Introduction
- Simulation studies
- Physical phantom studies
- Postmortem breast studies
- Patient studies

Meat study

Bin1 (22 ~ 40 keV) Bin2 (40 ~ 100 keV

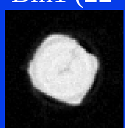

~ 30 m

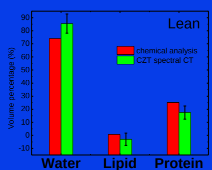

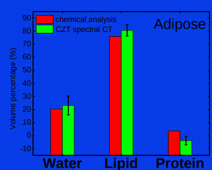

Post-mortem breast sample

Bin1 (22 ~ 42 keV) Bin2 (42 ~ 100 keV

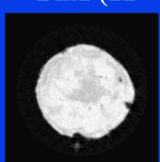

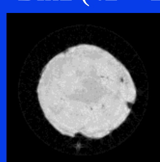

~ 100 mm

Three material decomposition of post-mo

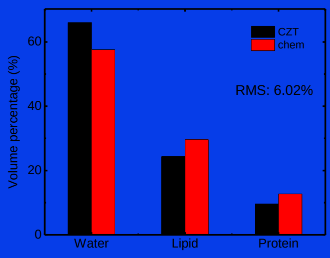

System requirements for patient studies

- Minimal time interval (less than 1 sec) between low and high energy images.
- Ability to switch kVp between low and high energy images (i.e. 28 kVp to 49 kVp).
- Ability to switch beam filter between low and high energy images (i.e. Rh filter to Cu filter).
- Negligible lag and ghosting between low and high energy images.

Conclusions

- Expected additional dose is low
- Proposed technique could be incorporated into existing screening mammography.
- Preliminary studies to date indicate the possibility of accurate breast density measurement in phantoms (within 3% error)

ACKNOWLEDGMENTS

This research was supported in part by Grant No. R01 CA136871 awarded by the NCI, DHHS.

Breast Density and Water Content

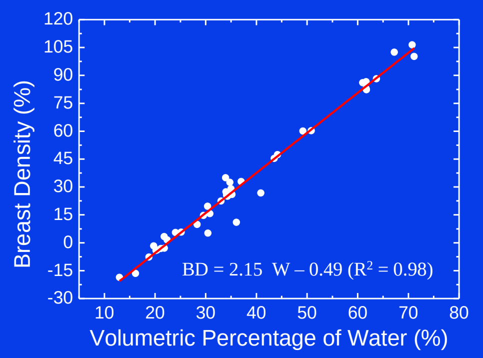

Breast Density and Lipid Content

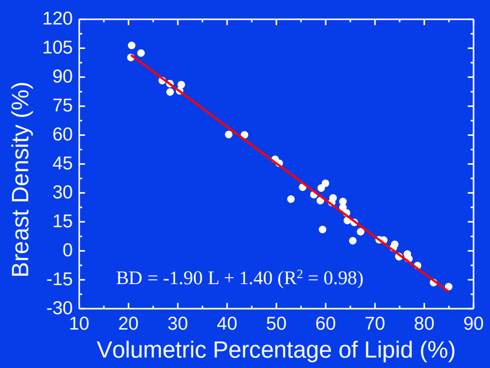

Breast Density and Protein Content

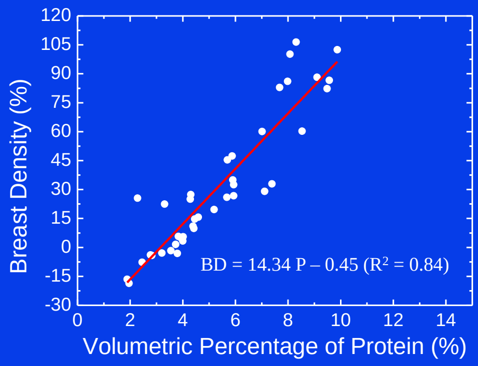

BI-RADS Reader Study

- IRB approval
- 93 patients
- 10 radiologists
- CC and MLO views
- Right and left breasts viewed in random order

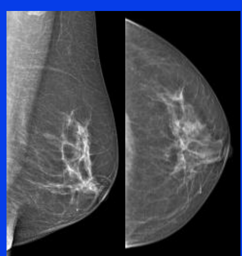

BI-RADS Ranking

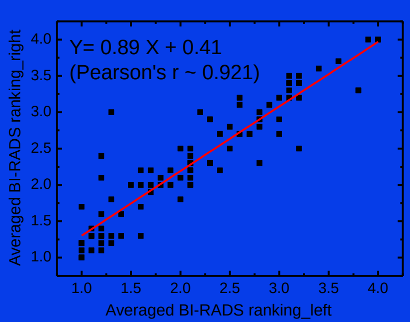

BI-RADS Breast Density

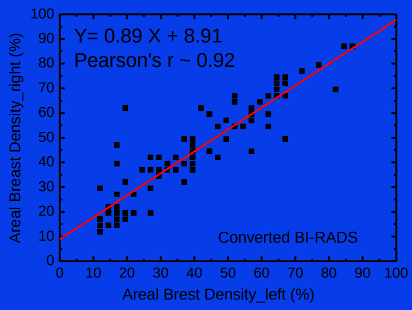

Observer Variability

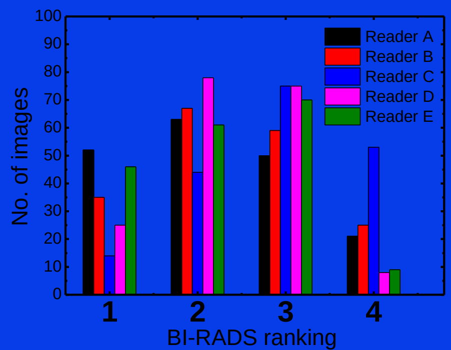

Histogram Thresholding

- Cumulus 4
- Two thresholds
- CC and MLO views in sequence
- Right and left blinded

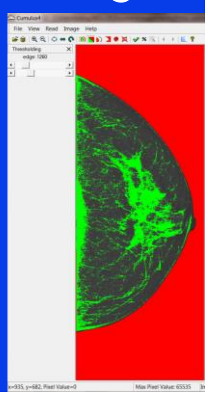

CC and MLO correlation from Cumulus

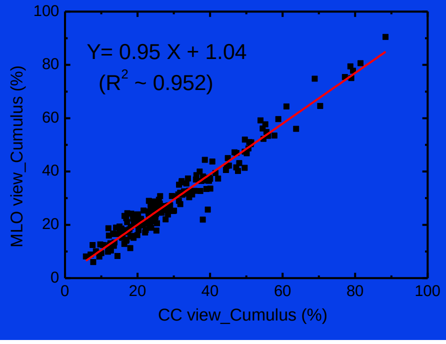

Right-left correlation from Cumulus

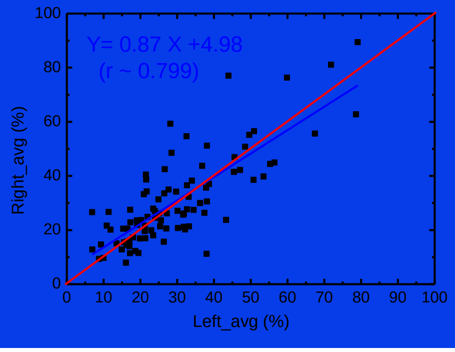

Fuzzy C-mean Clustering

- Automatic segmentation
- Total of 6 clusters
- First three clusters glandular tissue

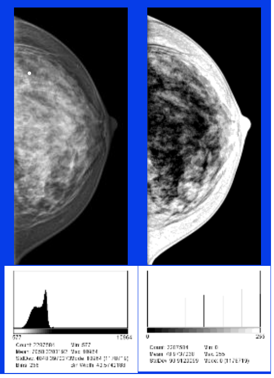

Automatic Segmentation using Fuzzy C-mean

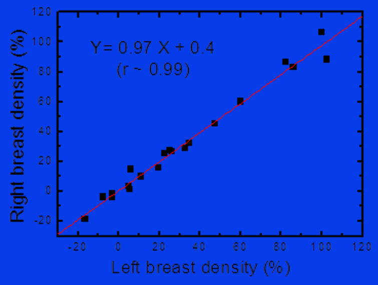

Dual Energy Decomposition

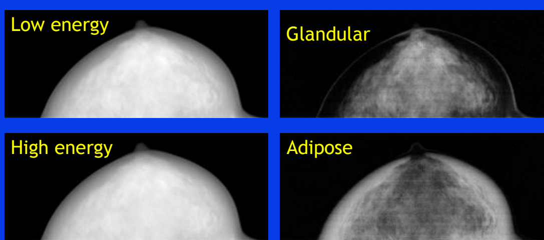

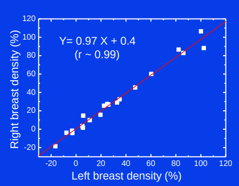

Fig 6: BD from DE right breast vs. left breast. BD from DE vs. %FGV from chemical analysis.

CC and MLO from dual energy

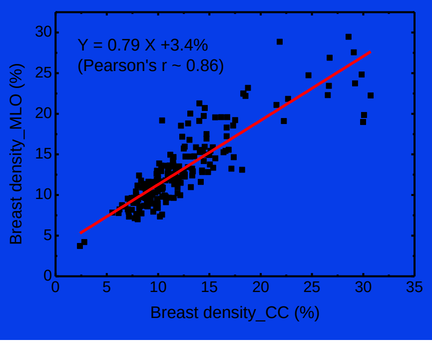

Breast Volume from Dual Energy

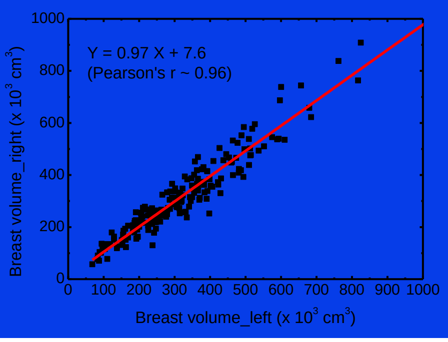

Breast Density from Dual Energy

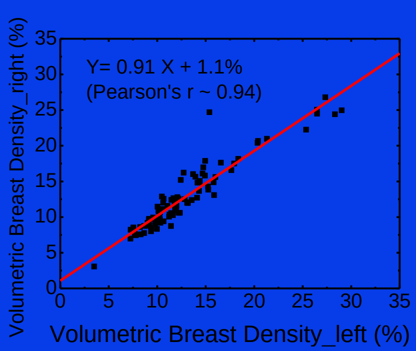

Conclusions

- Spectral mammography offers quantification of volumetric breast density with excellent precision.
- It largely eliminates the inter- and intra-observer variability in breast density estimation.

ACKNOWLEDGMENTS

This research was supported in part by Grant No. R01 CA136871 awarded by the NCI, DHHS.

Right-left Breast Correlations

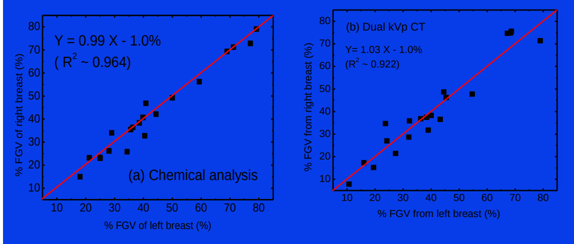

Breast Tissue Composition

Table 2. Density and elemental compositions of adipose tissue and glandular tissue used in theoretical investigations.

Tissue	H	C	N	O	Cl	Ca	Density (g/cc)	Ash (S,P,K,Ca)
Glandular		10.8%	3.2%	75.9%	-	-		
Tissue	10.2%	18.4%	3.2%	67.7%	-	-	1.04	0.5%
(Hammerstein[8])		30.5%	3.2%	55.2%	-	-		
Adipose		49.1%	1.7%	35.7%	-	-		
Tissue	11.2%	61.9%	1.7%	25.1%	-	-	0.93	0.1%
(Hammerstein[8])		69.1%	1.7%	18.9%	-	-		
Glandular	10.2%	15.8%	3.7%	69.8%	-	-	1.06	-
Tissue	10.6%	33.2%	3.0%	52.7%	-	-	1.02	-
(Woodard and White[10])	10.9%	50.6%	2.3%	35.8%	-	-	0.99	-
Adipose	11.2%	51.7%	1.3%	35.5%	-	-	0.97	-
Tissue	11.4%	59.8%	0.7%	27.8%	-	-	0.95	-
(Woodard and White[10])	11.6%	68.1%	0.2%	19.8%	-	-	0.93	-

Ducote J, Klopfer M and Molloi S, Volumetric lean percentage measurement using dual energy mammography, Med Phys, 2011 Aug;38(8):4498-504.

VLP Comparison

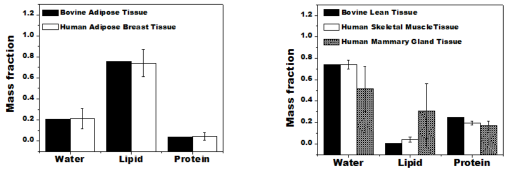

(a) (b)

Fig. 5. The data in this study are shown next to the data of Woodard and White. Note for the data in this study, the error bars were too small to be seen. The RMS difference for bovine adipose and human adipose tissues was 1.2%. The RMS difference for bovine lean and human skeletal muscle tissue was 0.4% and 22.2% for bovine lean and human mammary gland tissues.

Spectral Mammography

- Philips MicroDose Digital Mammography System
- Tungsten anode x-ray tube.
- Appropriate energy bin selection.
- No Scatter correction necessary

Dual Energy Decomposition

$$t_i = \frac{a_0 + a_1 l + a_2 h + a_3 l^2 + a_4 lh + a_5 h^2}{\sqrt{1 + b_1 l + b_2 h}}$$

Ducote J L , Molloi S, Quantification of breast density with dual energy mammography: An experimental feasibility study, Med. Phys. 37: 793, 2010.

VLP Comparison

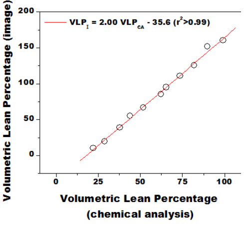

(a)

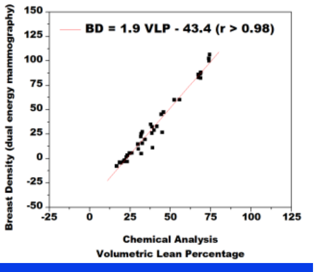

Breast Tissue Composition

Table 2. Density and elemental compositions of adipose tissue and glandular tissue used in theoretical investigations.

Tissue	H	C	N	O	Cl	Ca	Density (g/cc)	Ash (S,P,K,Ca)
Glandular Tissue (Hammerstein[8])	10.2%	10.8% 18.4% 30.5%	3.2% 3.2% 3.2%	75.9% 67.7% 55.2%	- - -	- - -	1.04	0.5%
Adipose Tissue (Hammerstein[8])	11.2%	49.1% 61.9% 69.1%	1.7% 1.7% 1.7%	35.7% 25.1% 18.9%	- - -	- - -	0.93	0.1%
Glandular Tissue (Woodard and White[10])	10.2% 10.6% 10.9%	15.8% 33.2% 50.6%	3.7% 3.0% 2.3%	69.8% 52.7% 35.8%	- - -	- - -	1.06 1.02 0.99	- - -
Adipose Tissue (Woodard and White[10])	11.2% 11.4% 11.6%	51.7% 59.8% 68.1%	1.3% 0.7% 0.2%	35.5% 27.8% 19.8%	- - -	- - -	0.97 0.95 0.93	- - -

Ducote J, Klopfer M and Molloi S, Volumetric lean percentage measurement using dual energy mammography, Med Phys, 2011 Aug;38(8):4498-504.

Breast Tissue Composition

Table 3. Summary of the apparent densities of breast tissue as compared to the composition determined from chemical analysis.

Composition Study Author	Tissue Type	Known Density	Range in Apparent Density	Average Apparent Density	RMS Error
Hammerstein[8]	Adipose Glandular	0 100	[−11.3 - 22.6] [84.6 - 136.5]	4.1 112.3	14.6 24.6
Woodard and White[10]	Adipose Glandular	0 100	[−7.6 - 26.4] [34.2 - 121]	9.0 74.6	16.5 43.8
Johns and Yaffe[11]	Adipose Glandular	0 100	[−31.8 - −18.5] [109.6 - 115.8]	−25.7 113.5	26.2 13.8

Breast Tissue Composition

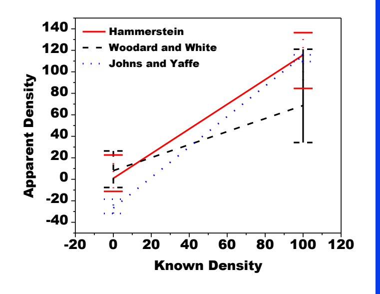

Volumetric lean percentage measurement using dual energy mammography
J Ducote, M Klopfer and S Molloi Med. Phys. (2011) AT-PRESS

Fig. 4 R&L

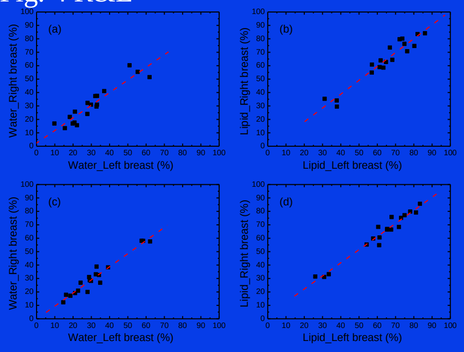
(a)
Water_Right breast (%)
Water_Left breast (%)
(b)
Lipid_Right breast (%)
Lipid_Left breast (%)
(c)
Water_Right breast (%)
Water_Left breast (%)
(d)
Lipid_Right breast (%)
Lipid_Left breast (%)